Supporting Information

Competitive adsorption of Cd(II), Cr(VI) and Pb(II) onto nano-maghemite: A spectroscopic and modeling approach

Michael Komárek [a*], Carla M. Koretsky [b], Krishna J. Stephen [b],

Daniel S. Alessi [c], Vladislav Chrastný [a,d]

[a] Department of Environmental Geosciences, Faculty of Environmental Sciences, Czech University of Life Sciences Prague, Kamýcká 129, Prague 6 – Suchdol, 165 21, Czech Republic

[b] Department of Geosciences, Western Michigan University, 1187 Rood Hall, Kalamazoo, MI 49008, USA

[c] Department of Earth and Atmospheric Sciences, University of Alberta, 1-26 Earth Sciences Building, Edmonton, Alberta, T6G 2E3, Canada

[d] Department of Geochemistry, Czech Geological Survey, Geologická 6, 152 00, Prague 5, Czech Republic

* Corresponding author, e-mail: komarek@fzp.czu.cz, tel.: +420224383857, fax: +4202343837

13 pages, 1 Text, 6 Tables, 3 Figures

Potentiometric titrations

Acid-base potentiometric titrations with 1 M HNO_3 and 1 M NaOH were performed in a CO_2-free chamber with N_2 as the inert gas and 0.01 M $NaNO_3$ as the background electrolyte. The nano-maghemite suspensions were titrated at 20 and 40 g/L. Hysteresis was observed during the forward and back titration at 20 g/L, but was significantly lower at 40 g/L. The obtained titration curves were also more reproducible at this w/v ratio. Therefore, the latter was used for the modeling. The equilibrium condition was set to a pH drift lower than 0.60 mV/h. Each forward and reverse titration took approximately 2.5 h in total. The laboratory temperature was maintained constant during the experiment.

Adsorption modeling

Data from the kinetic experiments were fitted to pseudo-first-order and pseudo-second-order equations:

$$\ln(q_e - q_t) = \ln q_e - k_1 t \quad (1)$$

$$\frac{t}{q_t} = \frac{1}{k_2 q_e^2} + \frac{1}{q_e} t \quad (2)$$

where k_1 (1/min) is the first-order adsorption rate constant, k_2 (g/µmol/min) is the second-order adsorption rate constant, q_e (µmol/g) is the adsorbed concentration of metal at equilibrium and q_t (µmol/g) the adsorbed concentration of metal at time t.

Langmuir (Eq. 3) and Freundlich (Eq. 4) isotherms were used to describe metal adsorption at equilibrium according to:

$$q_e = \frac{q_{max} K_L c_e}{1 + K_L c_e} \quad (3)$$

$$q_e = K_F c_e^n \quad (4)$$

where c_e is the equilibrium metal ion concentration in the solution after adsorption (μmol/L), q_e is the adsorbed metal concentration at equilibrium (μmol/g), q_{max} corresponds to the maximum sorption capacity (μmol/g), K_L is the Langmuir constant related to the energy of adsorption, K_F is a constant indicative of the relative adsorption capacity of the adsorbent and the constant n indicates the intensity of the adsorption. The model efficiency (E), which represents the proportion of regression, calculated from the error sum of squares, relative to the total sum of squares, was used to evaluate the fits. When $E = 1$, the data fit the model perfectly.

Isotope analyses

The double-spike method (^{111}Cd and ^{113}Cd, ^{50}Cr and ^{54}Cr enriched isotopes, Isoflex, USA) was applied before sample purification for mass bias correction. An interelement correction method based on adoption of a Tl spike solution (SRM NIST 997) was used to eliminate mass bias during Pb isotope measurement. The analytical sequence consisted of blank solution measurements between each sample and standard. The blank contained 2% HNO_3 and the measured intensities were subtracted from all samples and standards to obtain a baseline. Samples, standards and blanks were measured in 40 cycles and signals for each cycle were integrated for 4 s. NIST SRMs 3108, 979 and 981 standard solutions were analyzed every three samples. The isotope data for separate metals (Me) were related to this certified reference material as relative deviations in parts per mil (‰) according to:

$$\delta\ \mathrm{Me}\ (‰) = \left[\frac{\left({}^{heavier}\mathrm{Me}/{}^{lighter}\mathrm{Me}\right)_{measured}}{\left({}^{heavier}\mathrm{Me}/{}^{lighter}\mathrm{Me}\right)_{standard}} - 1\right] \times 1000 \quad (5)$$

Table S1 Aqueous species and stability constants used in surface complexation modeling in FITEQL (Visual MINTEQ 3.1 database).

Reaction	log K
$Cd^{2+} + H_2O \rightleftharpoons CdOH^+ + H^+$	-10.1
$Cd^{2+} + 2H_2O \rightleftharpoons Cd(OH)_2 + 2H^+$	-20.3
$Cd^{2+} + 3H_2O \rightleftharpoons Cd(OH)_3^- + 3H^+$	-33.3
$Cd^{2+} + 4H_2O \rightleftharpoons Cd(OH)_4^{2-} + 4H^+$	-47.3
$2Cd^{2+} + H_2O \rightleftharpoons Cd_2OH^{3+} + H^+$	-9.39
$Cd^{2+} + HCO_3^- \rightleftharpoons CdCO_3 + H^+$	4.37
$Cd^{2+} + 2HCO_3^- \rightleftharpoons Cd(CO_3)_2^{2-} + 2H^+$	7.23
$Cd^{2+} + HCO_3^- \rightleftharpoons CdHCO_3^+$	11.8
$Cd^{2+} + NO_3^- \rightleftharpoons CdNO_3^+ + H^+$	0.50
$CrO_4^{2-} + H^+ \rightleftharpoons HCrO_4^-$	6.51
$CrO_4^{2-} + 2H^+ \rightleftharpoons H_2CrO_4$	6.31
$2CrO_4^{2-} + 2H^+ \rightleftharpoons Cr_2O_7^{2-} + H_2O$	14.6
$CrO_4^{2-} + Na^+ \rightleftharpoons NaCrO_4^-$	0.70
$CrO_4^{2-} + K^+ \rightleftharpoons KCrO_4^-$	0.57
$Pb^{2+} + H_2O \rightleftharpoons PbOH^+ + H^+$	-7.60
$Pb^{2+} + 2H_2O \rightleftharpoons Pb(OH)_2 + 2H^+$	-17.1
$Pb^{2+} + 3H_2O \rightleftharpoons Pb(OH)_3^- + 3H^+$	-28.1
$2Pb^{2+} + H_2O \rightleftharpoons Pb_2OH^{3+} + H^+$	-6.40
$3Pb^{2+} + 4H_2O \rightleftharpoons Pb_3(OH)_4^{2+} + 4H^+$	-23.9
$4Pb^{2+} + 4H_2O \rightleftharpoons Pb_4(OH)_4^{4+} + 4H^+$	-20.9
$Pb^{2+} + HCO_3^- \rightleftharpoons PbCO_3 + H^+$	-6.53
$Pb^{2+} + 2HCO_3^- \rightleftharpoons Pb(CO_3)_2^{2-} + 2H^+$	9.94
$Pb^{2+} + HCO_3^- \rightleftharpoons PbHCO_3^+$	13.2
$Pb^{2+} + NO_3^- \rightleftharpoons PbNO_3^+ + H^+$	1.17
$H^+ + OH^- \rightleftharpoons H_2O$	-14.0
$H^+ + CO_3^{2-} \rightleftharpoons HCO_3^-$	10.3
$2H^+ + CO_3^{2-} \rightleftharpoons H_2CO_3$	16.7
$Na^+ + H^+ + CO_3^{2-} \rightleftharpoons NaHCO_3$	10.0

$$Na^{+} + CO_3^{2-} \rightleftharpoons NaCO_3^{-} \qquad 1.27$$

Table S2 Pseudo-first and pseudo-second order kinetic parameters of metal adsorption onto nano-maghemite at various pH values and in 0.01 M $NaNO_3$ as background electrolyte; k_1, k_2 – kinetic constants, q_e – adsorbed concentration of metal at equilibrium.

		Pseudo-first order			Pseudo-second order		
	pH	k_1 (g/µmol/min)	q_e (µmol/g)	R^2	k_2 (g/µmol/min)	q_e (µmol/g)	R^2
Cd(II)	6	n.a.	n.a.	n.a.	n.a.	n.a.	n.a.
	7	0.049	24.6	0.91	0.003	49.4	0.99
	8	0.049	29.8	0.96	0.004	50.5	1.00
Cr(VI)	3	0.070	23.9	0.88	0.005	48.4	1.00
	4.5	0.034	8.99	0.94	0.016	36.8	1.00
	6	0.055	9.93	0.78	0.013	34.2	1.00
Pb(II)	3	n.a.	n.a.	n.a.	n.a.	n.a.	n.a.
	4.5	0.035	10.9	0.74	0.002	21.6	0.86
	6	0.045	17.5	0.95	0.007	45.8	1.00

Table S3 Isotherm parameters of metal adsorption onto nano-maghemite at various pH values and in 0.01 M $NaNO_3$ as background electrolyte. The modeled data excluded the precipitation of otavite and hydrocerrusite (Fig. 3); K_L, K_F, n – isotherm constants, q_{max} – maximum sorption capacity, E – model efficiency.

Single-metal

		Langmuir			Freundlich		
	pH	K_L (L/g)	q_{max} (mmol/g, μmol/m^2)	E	K_F (L/g)	n	E
Cd(II)	3	n.a.	n.a.	n.a.	n.a.	n.a.	n.a.
	4.5	n.a.	n.a.	n.a.	n.a.	n.a.	n.a.
	6	0.886	0.011, 0.247	0.976	0.005	0.728	0.972
	7	47.42	0.011, 0.247	0.825	0.013	0.246	0.776
	8	59.00	0.018, 0.404	0.919	0.023	0.229	0.764
Cr(VI)	3	74.25	0.066, 1.480	0.971	0.076	0.211	0.956
	4.5	46.16	0.054, 1.211	0.965	0.061	0.218	0.965
	6	204.4	0.008, 0.179	0.883	0.009	0.139	0.594
Pb(II)	3	1.221	0.110, 2.466	0.951	0.052	0.467	0.869
	4.5	1.925	0.135, 3.027	0.974	0.079	0.506	0.920
	6	3.129	0.216, 4.483	0.915	0.182	0.440	0.986

Multi-metal (Cd(II)+Pb(II))

Cd(II)	6	n.a.	n.a.	n.a.	n.a.	n.a.	n.a.
	7	12.59	0.011, 0.247	0.959	0.011	0.321	0.855
	8	41.93	0.023, 0.516	0.901	0.027	0.239	0.729
Pb(II)	3	1.552	0.096, 2.152	0.908	0.050	0.426	0.807
	4.5	3.589	0.145, 3.251	0.998	0.100	0.345	0.949
	6	2.396	0.211, 4.731	0.943	0.165	0.544	0.982

Table S4 Isotope fractionation of Cd, Cr and Pb after the adsorption at pH values corresponding to maximum sorption according to the data obtained from isotherm modeling (Cd(II) pH 8, Cr(VI) pH 3, Pb(II) pH 6 and in 0.01 M $NaNO_3$ as background electrolyte, n = 3).

	Before adsorption	After adsorption
$\delta^{114}Cd_{NIST3108}$	-0.088 ± 0.012	-0.109 ± 0.008
$\delta^{53}Cr_{NIST979}$	0.016 ± 0.032	-0.053 ± 0.065
$\delta^{206}Pb_{NIST981}$	0.051 ± 0.022	0.091 ± 0.036

Table S5 log K values obtained from individual adsorption edges at various metal concentrations and ionic strengths using FITEQL.

$\equiv FeOH + Cd^{2+} \rightleftharpoons \equiv FeOCd^{+} + H^{+}$

Metal concentration	Ionic strength	log K	WSOS/DF
10^{-6} M	0.001 M	-1.144	0.009
10^{-6} M	0.01 M	-2.263	0.000
10^{-6} M	0.1 M	-2.385	0.001
10^{-5} M	0.001 M	-2.232	0.368
10^{-5} M	0.01 M	-2.730	0.370
10^{-5} M	0.1 M	-2.926	0.936

$\equiv FeOH + H^{+} + CrO_4^{2-} \rightleftharpoons \equiv FeCrO_4^{-} + H_2O$

Metal concentration	Ionic strength	log K	WSOS/DF
10^{-6} M	0.001 M	10.816	0.005
10^{-6} M	0.01 M	12.124	0.004
10^{-6} M	0.1 M	12.069	0.008
10^{-5} M	0.001 M	n.a.	n.a.
10^{-5} M	0.01 M	12.713	0.777
10^{-5} M	0.1 M	12.588	0.084

$\equiv FeOH + Pb^{2+} \rightleftharpoons \equiv FeOPb^{+} + H^{+}$

Metal concentration	Ionic strength	log K	WSOS/DF
10^{-6} M	0.001 M	5.000	0.001
10^{-6} M	0.01 M	3.445	0.006
10^{-6} M	0.1 M	3.569	0.005
10^{-5} M	0.001 M	4.074	0.291
10^{-5} M	0.01 M	2.385	0.256
10^{-5} M	0.1 M	1.471	0.051

Table S6 Beam-induced reduction of Cr(VI) to Cr(III) on Cr-sorbed nano-maghemite in the synchrotron X-ray beamline. The % Cr(VI) and % Cr(III) were calculated by linear combination fitting (LCF) of a time series of 9 sample scans (see Figure S2a) using Cr(VI) and Cr(III) standards. These data were used to fit a first-order kinetics model (Fig. S3) to determine that all Cr initially sorbed to the nano-maghemite was hexavalent.

XAS Scan #	Time elapsed (min)	% Cr(VI) - LCF	% Cr(III) - LCF	% Cr(VI) - rate equation fit
0	0			100
1	48.9	86.3	13.7	85.9
2	97.7	72.4	27.6	73.9
3	146.6	62.1	37.9	63.5
4	195.5	54.6	45.4	54.6
5	244.3	47.9	52.1	46.9
6	293.2	40.8	59.2	40.3
7	342.1	34.9	65.1	34.6
8	390.9	31.0	69.0	29.8
9	439.8	27.0	73.0	25.6

Rate const (min^{-1})	t (1/2) (min)
0.0031	223.6

Figure S1 XPS spectra of Fe(III) and Cd(II), Cr(VI) and Pb(II) adsorbed onto nano-maghemite at pH values corresponding to maximum sorption (Cd(II) pH 8, Cr(VI) pH 3, Pb(II) pH 6 and 0.01 M $NaNO_3$ as background electrolyte).

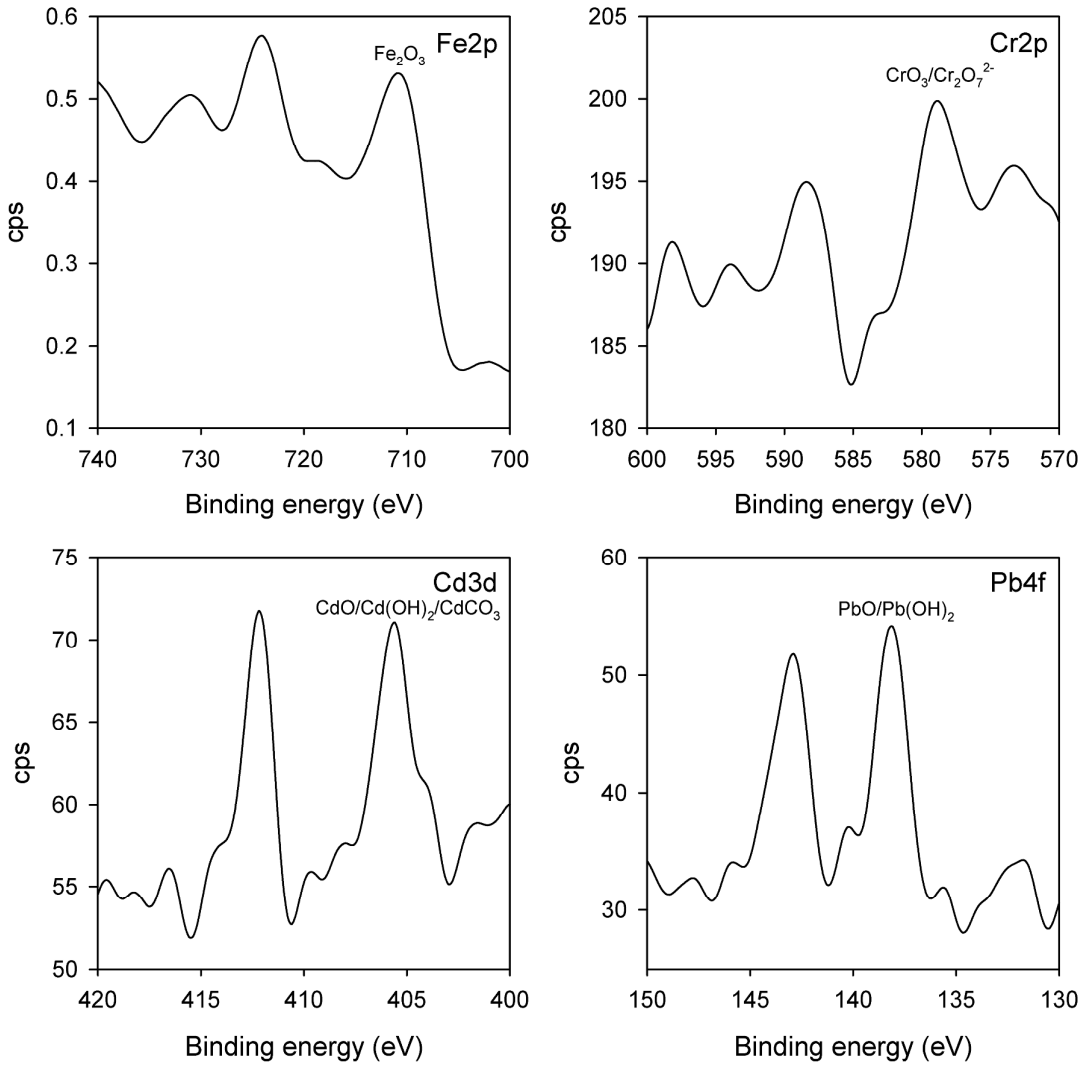

Figure S2 (a) Cr K-edge XANES of Cr-sorbed nano-maghemite, showing 9 sequential scans. The initial scan (brown spectrum) indicates 86.3% of the total Cr is hexavalent (see also Table S3) after 48.9 minutes of analysis (one scan time). Progressive scans show further Cr(VI) oxidation, as indicated by spectral changes such as a shrinking of the feature (peak) at 5994 eV that is indicative of Cr(VI). 73% of the total Cr is reduced to Cr(III) after 9 scans (yellow spectrum); (b) Fe K-edge XANES analyses on nano-maghemite with and without adsorbed Cr(VI); (c) linear combination fitting of 9 Cr K-edge scans, showing progressive reduction of Cr(VI) to Cr(III). Black dashed lines indicate fit, and results of fit appear in Table S3. Experiments prepared by adsorbing Cr(VI) onto nano-maghemite at pH 3 corresponding to maximum sorption and using 0.01 M $NaNO_3$ as background electrolyte.

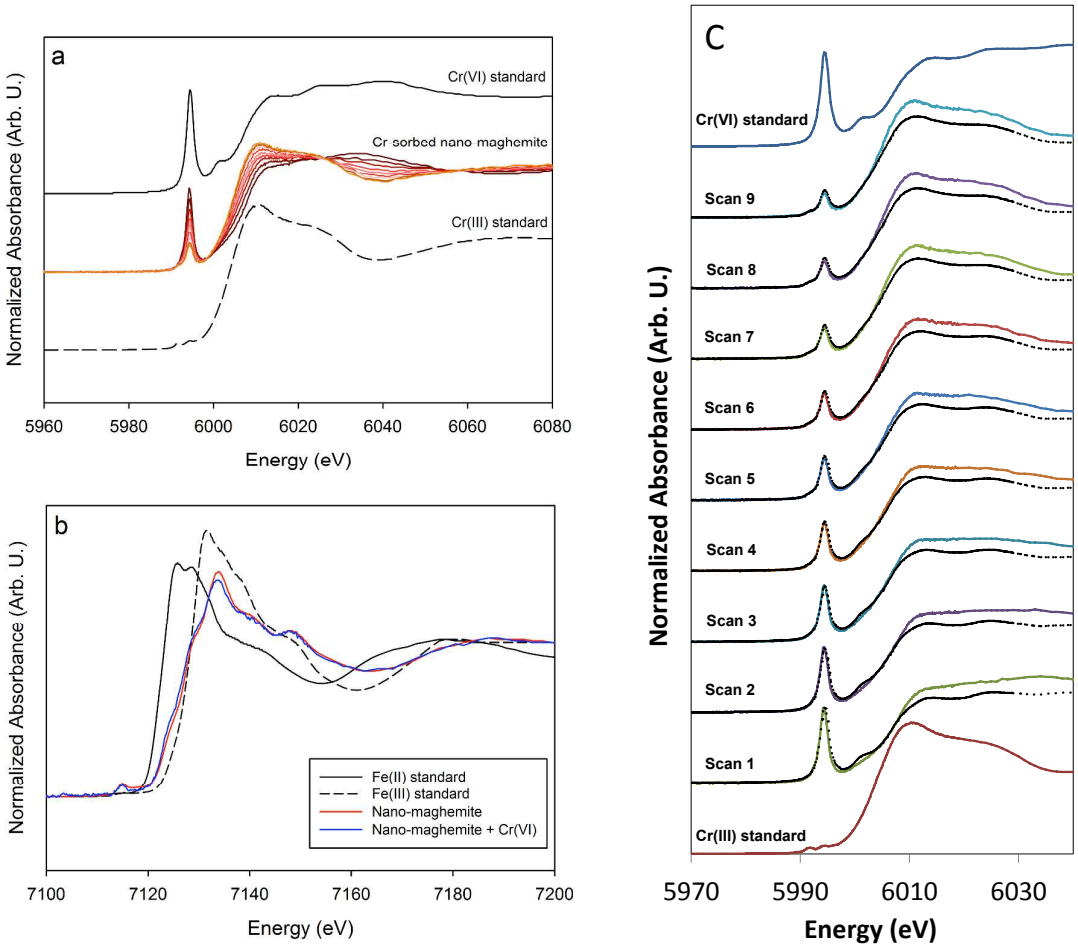
a
Cr(VI) standard
Cr sorbed nano maghemite
Cr(III) standard
Normalized Absorbance (Arb. U.)
5960
5980
6000
6020
6040
6060
6080
Energy (eV)
b
Fe(II) standard
Fe(III) standard
Nano-maghemite
Nano-maghemite + Cr(VI)
Normalized Absorbance (Arb. U.)
7100
7120
7140
7160
7180
7200
Energy (eV)
C
Cr(VI) standard
Scan 9
Scan 8
Scan 7
Scan 6
Scan 5
Scan 4
Scan 3
Scan 2
Scan 1
Cr(III) standard
Normalized Absorbance (Arb. U.)
5970
5990
6010
6030
Energy (eV)

Figure S3 First-order kinetics model of the reduction of Cr(VI) on nano-maghemite, induced by the synchrotron X-ray beam. Each scan at the beamline was 48.9 min, and a total of 9 scans were collected. The first order rate constant is 0.0031 min^{-1}, yielding a half life of Cr(VI) reduction to Cr(III) of approximately 224 min. Extrapolating the rate equation to t = 0 indicates that all of the Cr adsorbed to the NM prior to XAS analysis was hexavalent. See Table S6 for data.